

## Supporting Information

# Electric field-directed growth and photoelectrochemical properties of cross-linked Au–ZnO hetero-nanowire arrays

Teng Wang,<sup>a</sup> Bingjun Jin,<sup>a</sup> Zhengbo Jiao,<sup>a</sup> Gongxuan Lu,<sup>a</sup> Jinhua Ye,<sup>b</sup> and Yingpu Bi<sup>\*a</sup>

<sup>a</sup>State Key Laboratory for Oxo Synthesis & Selective Oxidation, and National Engineering Research Center for Fine Petrochemical Intermediates, Lanzhou Institute of Chemical Physics, CAS, Lanzhou 730000, China. E-mail: yingpubi@licp.cas.cn

<sup>b</sup> TU-NIMS Joint Research Center, School of Materials Science and Engineering, Tianjin University, 92 Weijin Road, Nankai District, Tianjin 300072, China.

## Experimental Section

### 1. Materials

All the chemicals were of analytical grade and used as received without any further purification, unless otherwise stated. Moreover, all chemicals were purchased from Sinopharm Group Chemical Reagent Co. Ltd. China. Deionized water with a resistivity of 18.25 MΩ.cm was used in all reactions. Indium-tin oxide (ITO)-coated glasses were purchased from Zhuhai Kaivo Electronic Components Co., Ltd. China.

### 2. Preparation of 3D cross-linked Au/ZnO heterostructures

The final product was prepared through two steps-the fabrication of the ZnO nanowire arrays via hydrothermal method and the synthesis of Au nanowire bonded ZnO nanowire arrays through a photo-assisted electrochemical deposition process.

#### 2.1 Preparation of ZnO nanowire arrays.

The ZnO nanowire arrays were synthesized via the method employed in our previous report. Firstly, 1.2 M zinc acetate dehydrate [Zn(CH<sub>3</sub>COO)<sub>2</sub>·2H<sub>2</sub>O] dissolved in ethylene glycol monomethyl ether [CH<sub>3</sub>O-CH<sub>2</sub>-CH<sub>2</sub>OH] with equal amount of diethanolamine (DEA) was added. After 30 min stirring, the as-prepared sol was sealed and put for 2 days. Then the obtained sol was spin-coated on an ITO substrate using a vacuum spin coater (VTC-100) followed by a 15 min, 150 °C drying procedure. After the repeated spin-coating process, the coated thin film was sintered in a muffle furnace in the air at 350 °C for 30 min to obtain the ZnO seed layer. Then the seeded substrate with the coating side upside-down was put into the growing solution of the ZnO nanowire arrays, which contained 0.04 M zinc nitrate (Zn(NO<sub>3</sub>)<sub>2</sub>·6H<sub>2</sub>O) and the equal amount of hexamethylene tetraamine (HMTA). The solution was put in a Teflon liner stainless-steel

autoclave to grow ZnO nanowire arrays at 95 °C for 6 h. Moreover, the final product was taken from the autoclave and intensively rinsed with deionized water and absolute ethyl alcohol for several times followed by a drying step in an oven at 60 °C.

## **2.2 Preparation of 3D cross-linked Au/ZnO nanowire arrays.**

The Au nanowire bonded ZnO nanowire arrays were prepared through a photo-assisted electrochemical deposition procedure. The deposition was realised through a typical 3-electrode system with a piece of Pt foil (3×2cm) as counter electrode, the saturated calomel electrode (SCE) as reference electrode and the as-prepared ZnO nanowire array as the working electrode. The electrodes were immersed in 0.4 mM HAuCl<sub>4</sub>, 0.1 M Na<sub>3</sub>PO<sub>4</sub> and 0.3 M Polyvinylpyrrolidone (PVP) aqueous solution, which were then illuminated by a 300 W Xe lamp (HSX-F/UV 300) for 2 minutes under certain bias voltages. After that, the products were taken out of the solution, rinsed with deionized water and absolute ethyl alcohol for several times to remove the residual and dried at 60 °C in the air.

## **3. Characterization.**

The morphology and elemental distributions of the products are characterized by field emission scanning electron microscope (FESEM, JSM-6701F, JEOL) employing an accelerating voltage of 5.00 kV with an energy dispersive spectrometer (EDS). X-ray diffraction analysis (XRD, Rigaku RINT-2000) using Cu K $\alpha$  radiation at 40 k eV and 40 mA was employed to identify the crystalline structure of our as-prepared products. X-ray photoelectron spectroscopy (XPS) was performed by a ESCALAB250xi photoelectron spectrometer with X-Ray Monochromatisation as the excitation source to analyze samples' elemental composition. The UV-Vis absorption spectra were carried out with a spectrophotometer (UV-2550, SHIMADZU, Japan). And the Photoluminescence (PL) spectra are measured at room temperature using an F-7000 spectrofluorometer (Hitachi High-Technologies, Tokyo, Japan) with the excitation wavelength (EX) fixed at 325 nm.

## **4. Characterization of Photoelectrochemical Performances**

The visible light photoelectrochemical properties of the as-prepared products were measured through a typical 3-electrode system, in which a piece of Pt foil (3×2cm) and a saturated calomel electrode (SCE) were used as counter and reference electrodes, respectively. And the as-prepared ZnO nanowire array and 3D cross-linked Au/ZnO hybrids were employed to be the working electrodes with a surface area of 2 cm<sup>2</sup>, respectively. The whole photoelectrochemical tests were

operated in 0.1 M Na<sub>2</sub>SO<sub>4</sub> aqueous solution and recorded by an electrochemical workstation (CHI660D). A 300 W Xe lamp (HSX-F/UV 300) with an ultraviolet-cut filter was used as the resource of visible light illumination. Linear sweep voltammograms were measured under a bias voltage between 0 V and +0.8 V (vs.SCE) with a scan rate of 0.1 V/s under chopped light irradiation. Amperometric i-t curves were tested at a bias voltage of +0.4 V (vs. SCE).

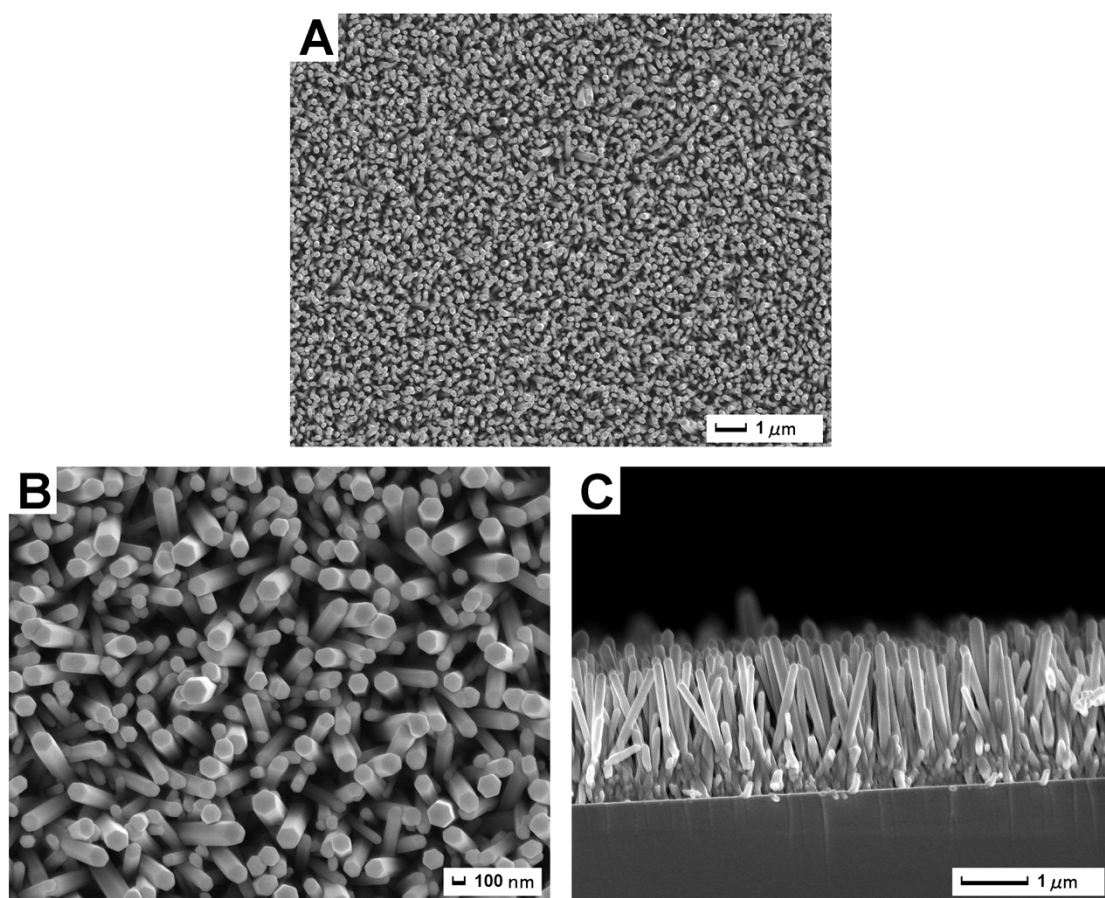


Fig. S1 Top-view (A, B) and cross-sectional (C) SEM images of ZnO nanowire arrays

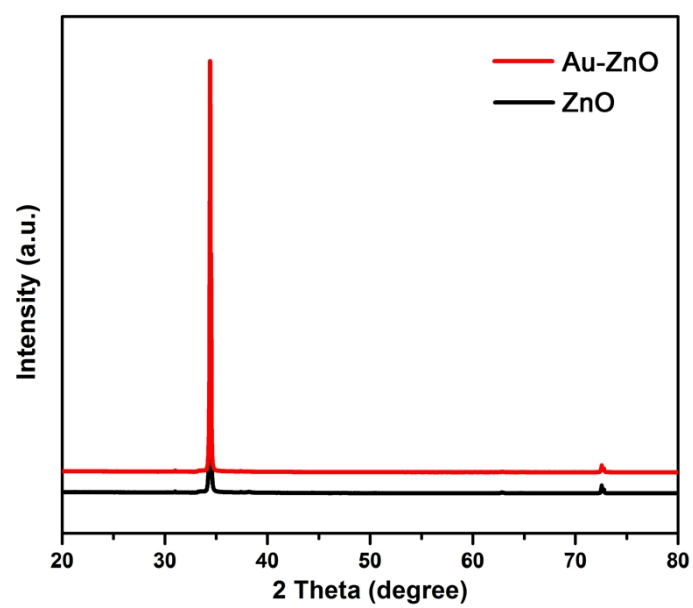


Fig. S2 XRD patterns of ZnO nanowire arrays and Au/ZnO heterostructures

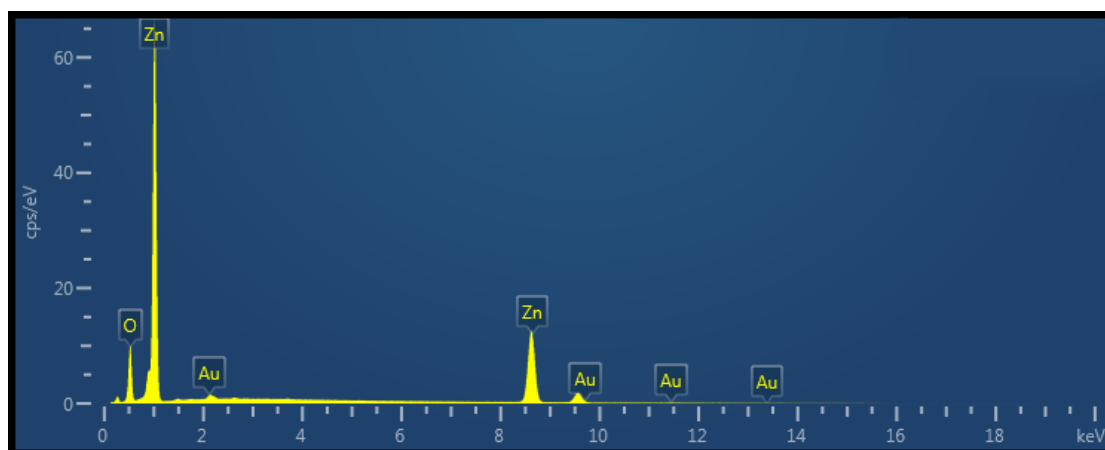


Fig. S3 EDS of Au/ZnO nanohybrids

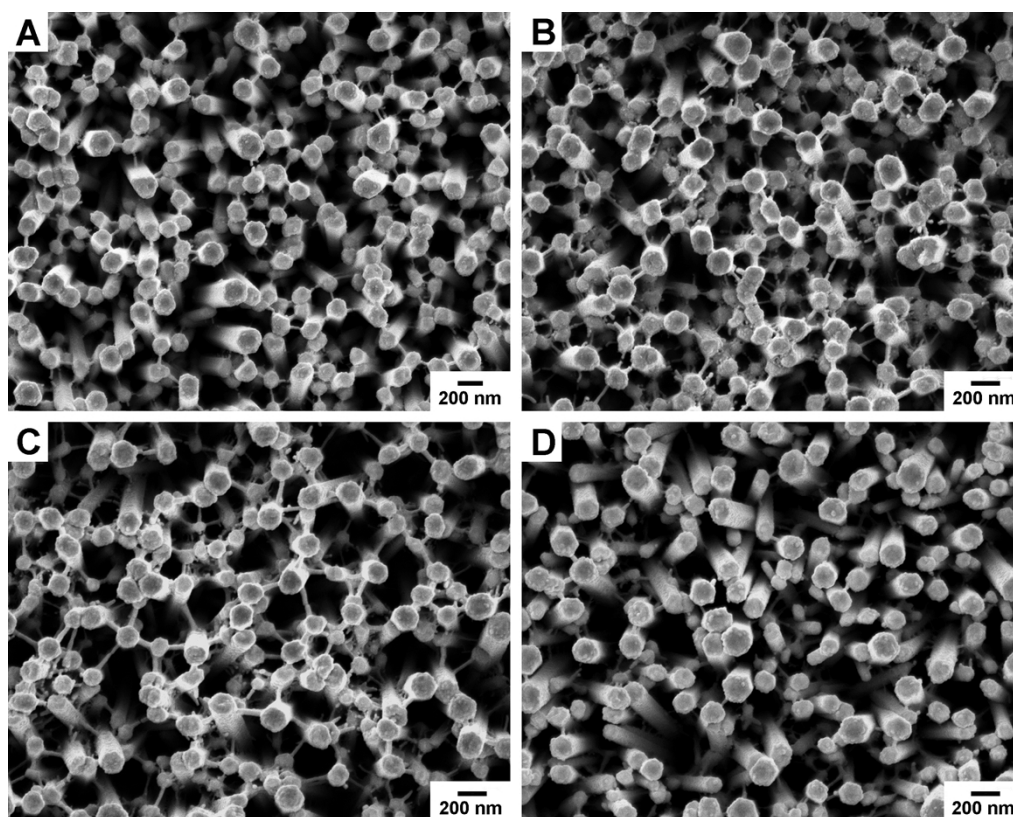


Fig. S4 Top-view SEM images of Au/ZnO nanowire arrays synthesized at voltage of 0 V (A), +0.1 V (B), +0.2 V (C) and +0.4 V (D) vs. SCE.

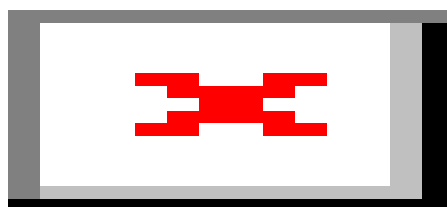


Fig. S5 SEM images of cross-linked Au/ZnO nanowire arrays obtained without light irradiation.

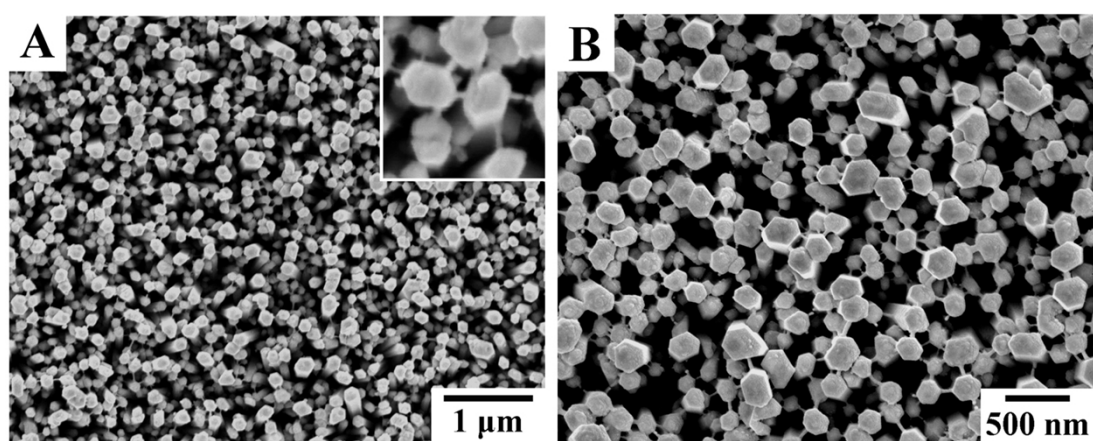


Fig. S6 SEM images of cross-linked Au/ZnO nanowire arrays obtained without bias voltage.

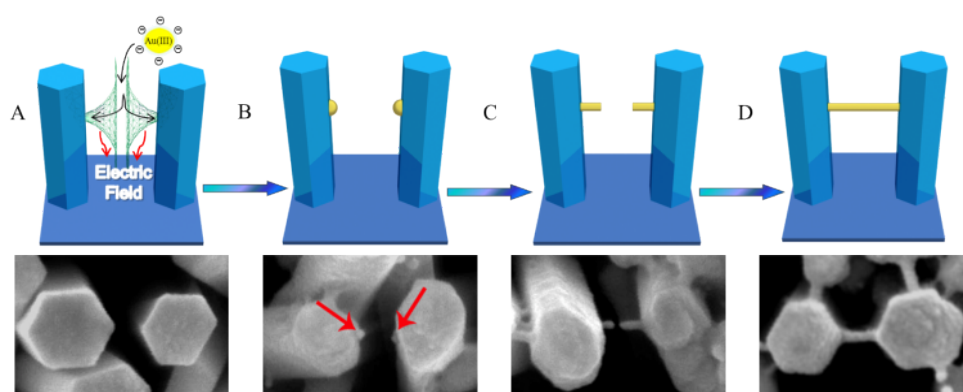


Fig. S7 Schematic illustration and SEM images of the formation process of cross-linked Au/ZnO nanowire arrays



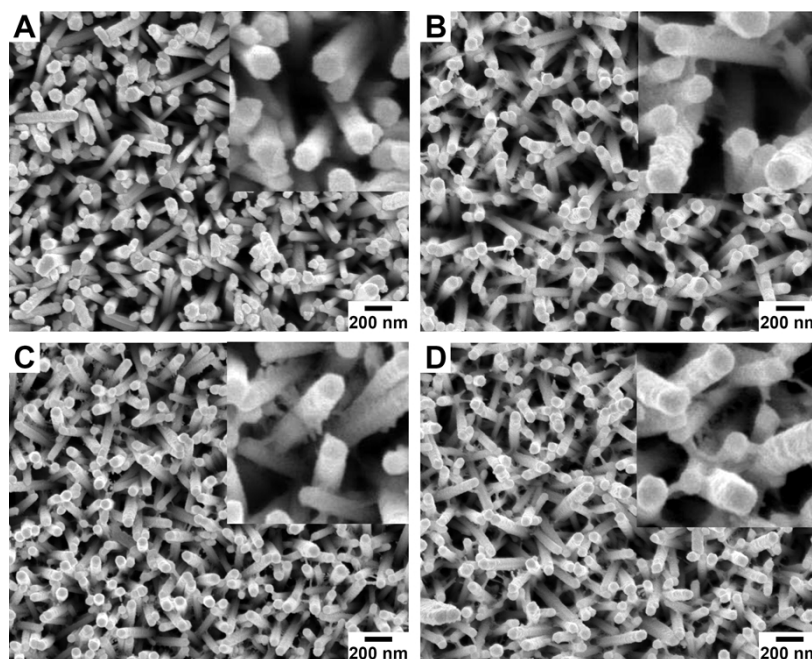


Fig. S8 Au/ZnO heterostructure with photodeposition time fixed at 20s (A), 40s (B), 60s (C), 80s (D), respectively

### The analysis of possible growth mechanism

Up to now, the photodeposition technique has been extensively used to prepare metal nanoparticles on semiconductor to form hetero-nanostructures. However, the controllable growth of Au nanowires over ZnO nanowires to construct cross-linked Au/ZnO hierarchical architecture under the electric field direction and photo-reduction has been rarely studied. To further explore this growth process, the morphology as well as structure evolutions of Au/ZnO nanoproducs obtained by adjusting the parameters has been investigated detailedly. As shown in Fig. S5, in the absence of photo-irradiation, Au nanowires could not be formed on ZnO nanowire arrays. However, when bias voltage was removed from the present process, interestingly, the Au nanowires were conventionally constructed on the ZnO nanowire arrays (Fig. S6), although their numbers were much lower than that of the sample obtained under bias voltage. These demonstrations clearly reveal that the anisotropic growth of Au nanowires in present system should be mainly ascribed to the photo-induced deposition, which is consistent with the individual photodeposition process. The corresponding growth process under photodeposition conditions had been studied previously and shown in Fig. S7.<sup>1</sup> More specifically, the photogenerated electrons and holes can be separated and accumulated on the top and side surface of ZnO nanowires, respectively. The enriched holes on the side surfaces of ZnO nanowires could generate a positive

electric field, which attracts negatively charged gold ions to the surface of two close ZnO nanowires. Simultaneously, the space locality with lowest distance from the neighboring ZnO nanowires generated the relatively strong electric field intensity, which could induce the simultaneous growth of Au nanorods from the opposite direction on ZnO nanowires and final formation of connective Au nanowires.

At present, we consider that the introduction of bias voltage could facilitate the formation process of Au nanowires on ZnO nanowire arrays. To further confirm this speculation, the same growth process as individual photodeposition was performed under the bias voltage of +0.2V. As shown in Fig. S8, due to the promotion effect of the bias potential, the growth of Au nanowires is very fast that numerous Au nanowires can be observed in only 40 seconds' deposition. However, as shown in the inset images, note that the similar growth steps can also be observed in a non-potential photodeposition process. Therefore, it can be confirmed that the photogenerated electric field induces the anisotropic growth of Au nanowires, while suitable bias voltage can significantly improve the growth of Au nanowires. Moreover, unlike the uncontrollable ability of photodeposition, the density of Au nanowires could be easily tailored by simply adjusting the bias voltage.

1. T. Wang, B. Jin, Z. Jiao, G. Lu, J. Ye and Y. Bi, *J. Mater. Chem. A*, 2014, 2, 15553-15559.

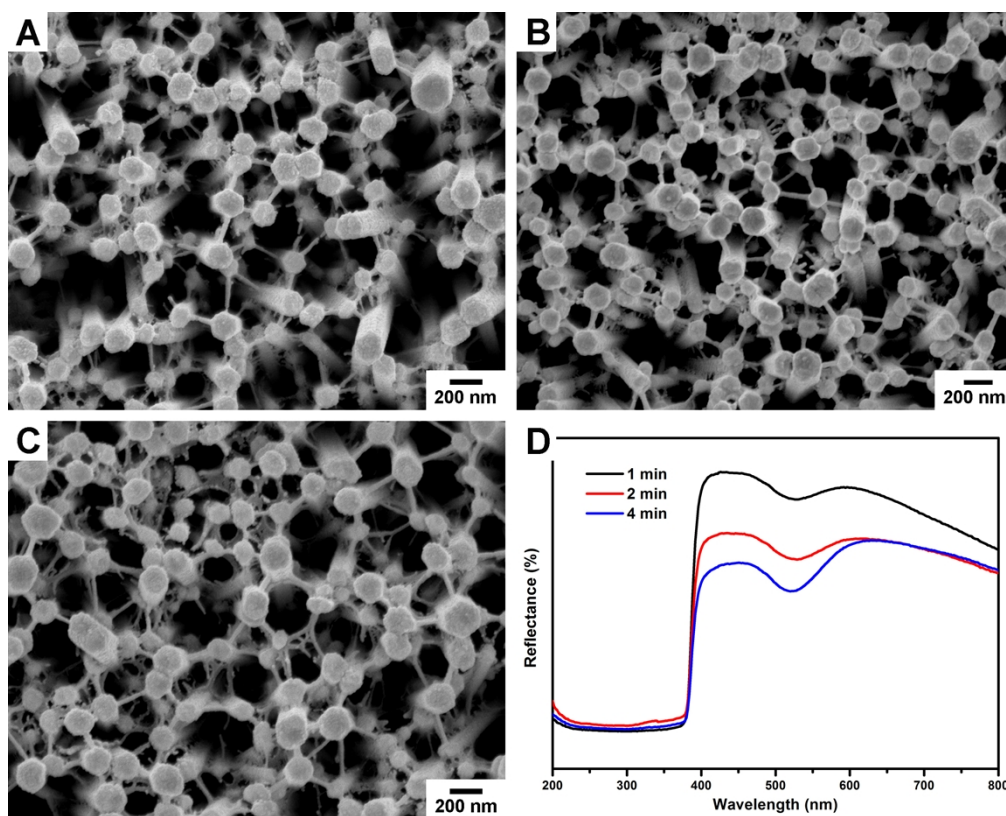


Fig. S9 Top-view SEM images of Au/ZnO nanowire arrays synthesized with irradiation time fixed at 1 min, 2 min, 4 min, respectively and their corresponded UV-vis light reflectance spectra.

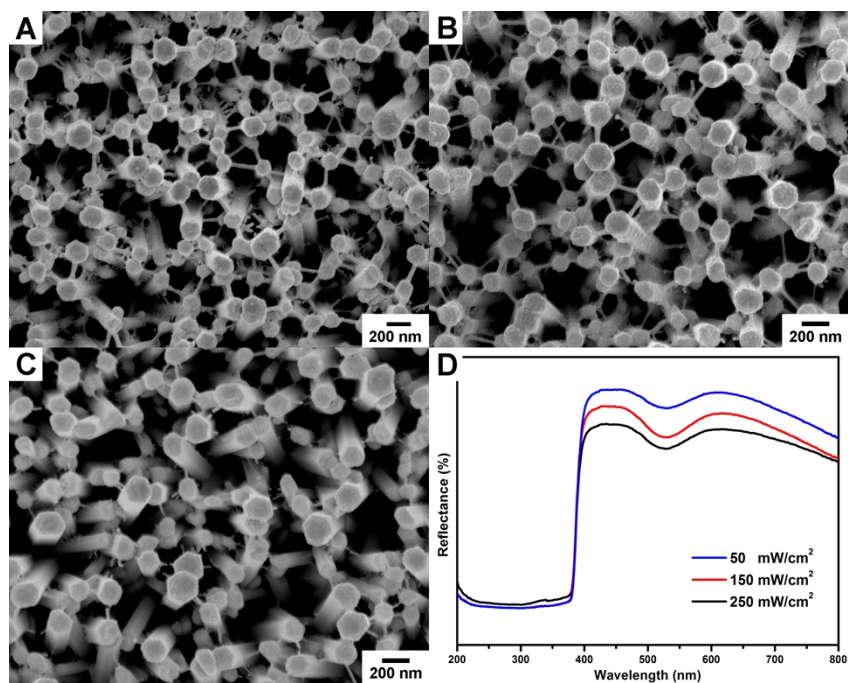


Fig. S10 Top-view SEM images of Au/ZnO nanowire arrays fabricated with irradiation power fixed at 250 mW cm<sup>-2</sup> (A), 150 mW cm<sup>-2</sup> (B), 50 mW cm<sup>-2</sup> (C), respectively and their corresponded UV-vis light reflectance spectra.

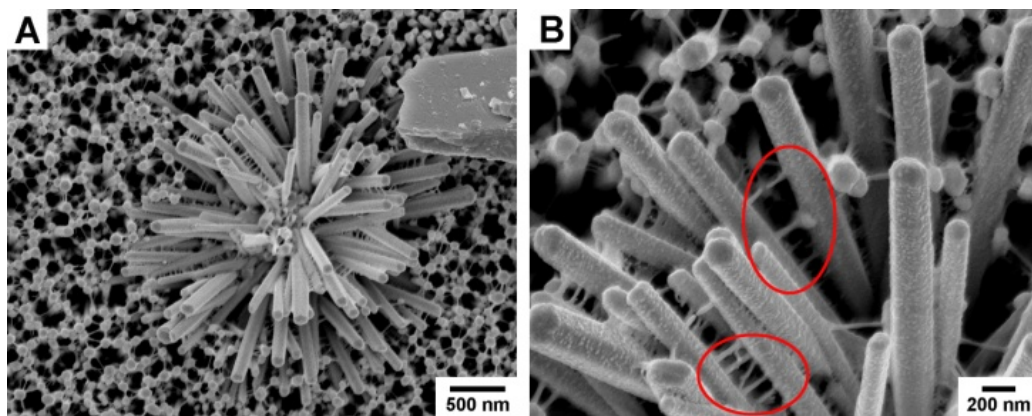


Fig. S11 Direction controls of Au nanowire growth

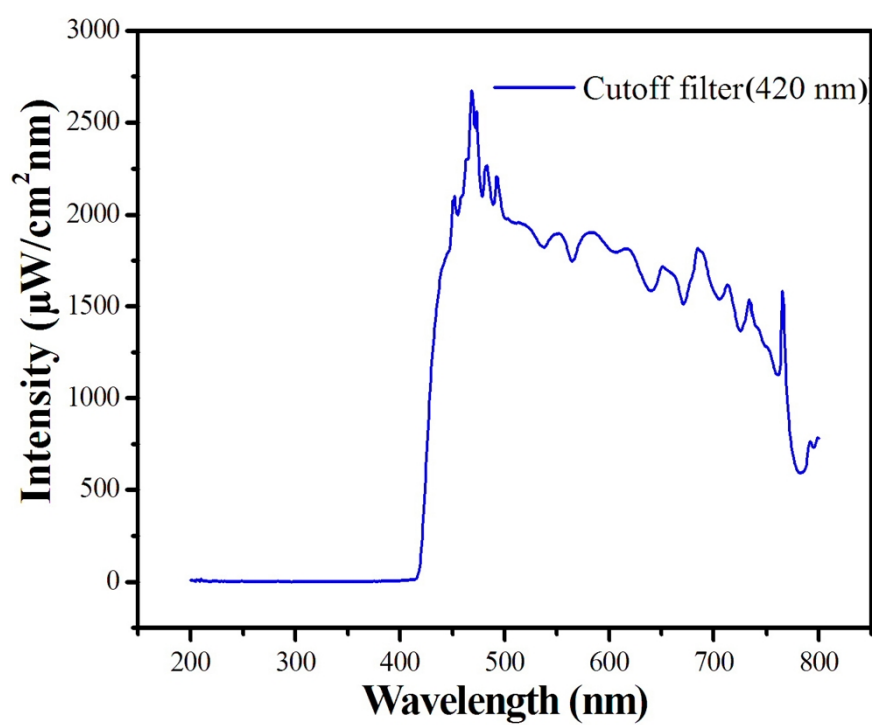


Fig. S12 The intensity and wavelength distribution of the irradiation light employed in the photoelectrochemical property tests. Integral intensities were measured under the actual experimental conditions.

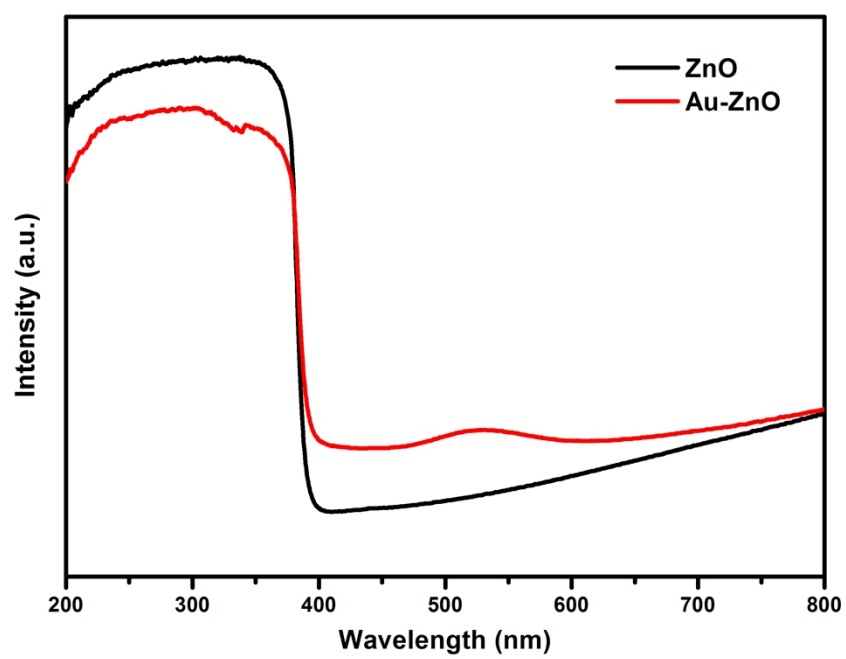


Fig. S13 Ultraviolet-visible diffusive reflectance spectrums of ZnO and Au/ZnO heterostructures